RSC Advances

PAPER

View Article Online
View Journal | View Issue

Cite this: *RSC Adv.*, 2020, **10**, 33566

Mechanism of the evolution of pore structure during the preparation of activated carbon from Zhundong high-alkali coal based on gas–solid diffusion and activation reactions

Dingcheng Liang, *[a] Qiang Xie,[a] Jinchang Liu,[a] Fei Xie,[b] Deqian Liu[a] and Chaoran Wan[a]

Zhundong coal can significantly reduce the preparation temperature of activated carbon (AC) due to the high contents of alkali and alkaline earth metals (AAEMs) present in it. Moreover, because of its lower operating temperature and the presence of carbon matrix, Zhundong coal can effectively inhibit the release of AAEM during the preparation of AC. For these reasons, the preparation of AC from Zhundong coal is a promising approach for the clean utilization of Zhundong coal. Accordingly, this study was aimed to investigate optimum conditions for the preparation of AC from Zhundong coal. For this purpose, at first, Raman spectroscopy was used to determine the conditions for an optimal carbonization process using a coal sample; then, the evolution of the pore structure of AC under different conditions was examined by small-angle X-ray scattering (SAXS) and the N_2 adsorption analyser. Furthermore, environmental scanning electron microscopy (ESEM) was performed to analyze the surface morphology of AC. Finally, by dividing the activation process into gas–solid diffusion and activation reactions, a mechanism for the evolution of pore structure during the preparation of AC was proposed. The results showed that the char with an amorphous structure and less graphite-like carbon, which was obtained by heating Zhundong coal from room temperature to 600 °C at 5 °C min^{-1} under the protection of N_2 and then maintaining it at this temperature for 60 min, is suitable for the subsequent activation process. At low temperatures, the diffusion of H_2O was dominant in the activation process, and the weak gas–solid reaction resulted in poor development of the pore structure; on the other hand, the CO_2 activation reaction mainly occurred on the surface of the char due to the poor diffusion of CO_2, and then, the produced pores could improve the diffusion of CO_2; this led to significant development of the pore structure. With an increase in temperature, the H_2O diffusion reaction was enhanced, and the pore structure of AC was completely developed; however, the diffusion of CO_2 reduced with an enhancement in the CO_2 activation reaction, leading to the consumption of carbon matrix by CO_2 gasification instead of pore formation by the CO_2 activation reaction. Therefore, proper utilization of the unique characteristics of H_2O and CO_2 during pore formation is important to control the activation process.

Received 13th July 2020
Accepted 25th August 2020

DOI: 10.1039/d0ra06105k

rsc.li/rsc-advances

1. Introduction

Zhundong coal field in Xinjiang Uygur Autonomous Region, as the largest integrated coal field in China, has the characteristics of stable storage, shallow burial, large thickness, simple geological structure, and easy mining.[1] However, owing to the complex coal-forming process, the content of alkali and alkaline earth metals (AAEMs) in Zhundong coal is high, and is similar to that of Victorian brown coal.[2,3] When Zhundong coals are directly used as fuels, these AAEMs cause severe corrosion, fouling, and ash deposition problems both inside the furnace and in the convective pass.[4] Moreover, numerous studies have indicated that a high content of AAEMs in coal can play a positive role in promoting the development of pores during the thermal processing of coal.[5] In addition, Zhundong coal has the features of low metamorphism, good reactivity, low ash production, and low sulfur content.[6] Due to these features, Zhundong coal can be used as a potentially ideal raw material for the preparation of porous carbon materials such as activated carbon (AC) and carbon nanomaterials.[7]

The preparation of AC may be difficult due to the high volatilization and release of AAEMs from the coal sample, which results in slagging and corrosion of the production equipment.

[a]*School of Chemical and Environmental Engineering, China University of Mining and Technology (Beijing), Beijing 100083, PR China. E-mail: liangdc@cumtb.edu.cn*
[b]*Beijing Synchrotron Radiation Facility, Institute of High Energy Physics, Chinese Academy of Sciences, Beijing, 100049, PR China*

Therefore, a comprehensive investigation on the preparation of AC from Zhundong coal is required. It is confirmed from the literature that temperature is the most important factor affecting the release of AAEMs from the coal surfaces.[8] Compared with the high temperature requirement for coal combustion and gasification, the temperature required for the preparation of AC is lower; thus, the amount of the AAEMs released by volatilization is less,[9,10] and the harm to the equipment can be easily controlled. Researchers have also found that the carbon matrix shows a significant inhibitory effect on the release of AAEMs from coal.[11,12] Therefore, the carbon skeleton present in Zhundong coal can effectively inhibit the volatilization and release of AAEMs during the preparation of AC from Zhundong coal. It can be concluded from these studies that a lower operating temperature and the presence of a carbon matrix can effectively inhibit the release of AAEMs from Zhundong coal during the preparation of AC.

Previously, the traditional production enterprises of AC used to be concentrated in Shanxi and Ningxia provinces of China. However, with the development of coal resources in Xinjiang, the AC industry has gradually started to move to the west of China, and Shenhua Xinjiang Energy Co. Ltd. built the largest AC production unit in the world in 2014. Due to the lack of a complete breakthrough in the regulation technology of the pore structure of AC, coal-based AC has the limitations of high output, few varieties, and low quality, which lead to low-price sales of this type of AC as the base carbon. Therefore, the distribution of pore structure is the most difficult factor in the preparation of AC. Based on this background, this study was aimed at using a Zhundong high-alkali coal sample as a raw material for the preparation of AC. Based on the carbonization control theory reported in a previous study, the coal was carbonized into char with an isotropic, difficult graphitized, and amorphous structure.[13] Then, according to the gas–solid diffusion and activation reaction, the evolution of pore structure was comprehensively explored under different conditions during the activation process. Thus, this study provides a theoretical basis for the targeted regulation of the pore structure of coal-based AC.

2. Experimental

2.1 Materials

Typical Zhundong high-alkali coal was employed in this study, and the properties of the coal sample were analyzed according to GB/T 476 and GB/T 212. Then, the coal sample was burned by gentle combustion at 500 °C to minimise the loss of the AAEMs species, and the composition of the ash was characterised by X-ray fluorescence spectrometry (XRF, Thermo Scientific, ARL PERFORM'X 4200). The results of the proximate and ultimate analysis of the coal sample and ash are presented in Table 1.

Table 1 Results of the analysis of the coal and ash samples[a]

Proximate analysis (wt%)				Ultimate analysis (wt%)				
M_{ad}	A_d	$V_{daf.}$	$FC_{daf.}$	$C_{daf.}$	$H_{daf.}$	$O_{daf.}$ (diff.)	$N_{daf.}$	$S_{t,d}$
10.13	4.17	30.93	69.07	70.54	3.57	24.43	0.69	0.77

Ash composition (wt%)									
SiO_2	Al_2O_3	Fe_2O_3	CaO	MgO	K_2O	Na_2O	SO_3	TiO_2	BaO
18.72	10.62	7.4	32.2	9.64	0.249	8.13	9.23	0.136	0.107

[a] *M*: moisture; *A*: ash; *V*: volatile matter; FC: fixed carbon; ad: air dry basis; d: dry basis; daf.: dry ash-free; diff.: by difference; and t: total.

2.2 Methods

2.2.1 Preparation of char and AC. A sub-bituminous coal sample obtained from Zhundong coalfield was employed in this study. The coal sample was ground in a mill until the particle size was less than 0.074 mm. Subsequently, the particles were pressed into pellets with a diameter of 25 mm and thickness of 8 mm under 200 MPa, and then, these pellets were crushed into 3–10 mm particles. Finally, the crushed coal briquettes were carbonized and activated in a tube furnace (Nabertherm, R50/500/12).

To determine the effect of temperature on the carbonization process, the carbonization experiments were performed in the temperature range from 450 to 600 °C in 50 °C increments under the following conditions: high-purity nitrogen was used as a carrier gas at a flow rate of 100 mL min^{-1} and the holding time was 45 min. In addition, the effect of the holding time on the structure of the char was investigated using different holding times, *i.e.* 30, 45, and 60 min, and the carbonization temperature was set to 600 °C. The corresponding samples were named as follows: temperature-char-holding time, for example, 600-char-45 indicates that the sample derived from Zhundong coal was carbonized at 600 °C at the holding time of 45 min.

The preparation of AC involves a carbonization process and an activation process. The procedure of carbonization is as follows: at first, the coal sample was heated to 600 °C under a N_2 atmosphere (100 mL min^{-1}) and held for 60 min. After the end of the holding time, steam (100 mL min^{-1}) and CO_2 (100 mL min^{-1}) were separately introduced into the tube furnace. Moreover, the reactor was continuously heated until the target temperature was reached and then held for 2 h. Due to the good reactivity of the Zhundong high-alkali coal, relatively low activation temperatures were used, *i.e.* 700, 750, 800, 850, and 900 °C. Finally, heating was stopped, and the reactor was naturally cooled under a nitrogen atmosphere. The AC sample was obtained and named according to the following rules: agent-temperature-AC. For example, H_2O-700-AC implies that the agent of AC is steam and the activation temperature is 700 °C. Note that the heating rate for both the carbonization and activation processes was 5 °C min^{-1}.

2.2.2 Sample characterization. Raman spectra of the coal and char samples were acquired using a Renishaw inVia confocal micro-Raman spectrometer. The excitation laser beam (532 nm wavelength) was focused on the sample by

a microscope, and the Raman signal was obtained in the backscattered direction. The power of the laser focused on the sample surface was controlled at about 1 mW. The Raman spectra were obtained in the range between 800 and 1800 cm^{-1}, and all the scans were performed three times. The GRAMS/32 AI software was used to deconvolute the Raman spectra into 10 Gaussian bands, and this process has been described in a previous study.[4]

Small-angle X-ray scattering (SAXS, Xenocs SA, Nano-inXider) refers to the phenomenon of X-ray scattering in a small angular range around the incident beam when X-ray irradiates a sample with electron density fluctuations on the nanometer scale; herein, the SAXS experiments were carried out to analyze the AC samples. The incident X-ray wavelength λ was 0.154 nm, and the detector-to-sample distance was 937.5 mm. The sample data was obtained in 10 min in an all-vacuum environment and was then background corrected and normalized using the standard procedure.

The pore structure parameters of the AC samples were examined using a nitrogen adsorption analyzer (Micromeritics, ASAP 2460). The specific surface area was calculated by the Brunauer–Emmett–Teller (BET) method.

Evaluations of the morphologies and surface compositions of the samples were conducted using environmental scanning electron microscopy (ESEM, Thermo Fisher, Quattro C).

3. Results and discussion

3.1 Determination of the carbonization conditions for AC

The excellent adsorption performance of AC is due to its large specific surface area.[14] Among all kinds of pores of AC, micropores have the greatest effect on the specific surface area and adsorption performance of AC,[15] and a micropore is essentially a molecular-sized gap between the bent and deformed aromatic ring layer in the microcrystalline structure of AC.[13] Previous studies have confirmed that the carbonization temperature, heating rate, and holding time can affect the microcrystalline structure of the char, and the initial pores are formed by the irregular stacking of these graphite layer fragments.[16,17] The initial pores in the char affect the subsequent activation process and change the pore structure development of AC.

Raman spectroscopy is an efficient method for investigating the degree of crystallinity, defects, and disorder in carbon materials.[18,19] Thus, it was used to explore the evolution of the structure of the char samples derived from Zhundong coal under different carbonization conditions to determine optimal conditions for achieving a char sample with an amorphous structure and abundant initial pores. It was possible to fully develop the pore structure in the subsequent activation stage. The Raman spectra with the corrected baseline for the raw coal and char samples in the 800–1800 cm^{-1} range and the ratio of the D band to G band peak areas of different samples are shown in Fig. 1.

In the Raman spectra, the D band represents a disordered structure and the G band confirms the presence of a graphitic structure.[20] Therefore, the band area ratio I_D/I_G is used as a significant parameter to investigate a crystalline structure or graphite-like carbon.[21,22] As shown in Fig. 1(b), when the holding time was kept constant and the carbonization temperature was increased, the ratio of I_D/I_G increased and reached a high point at 600 °C. Thus, in the following experiment, when the carbonization temperature was fixed at 600 °C and the holding time was changed, the ratio of I_D/I_G was proportional to the holding time. The reason for the above-mentioned phenomenon is the formation of polycyclic aromatic units by the condensation of the macromolecular network in the char with an increase in the carbonization temperature. During this process, the chemical bond between the macromolecular compounds is broken, and then, micromolecules are formed. These micromolecules deposited on the surface of the char, which resulted in a large number of defect structures and amorphous structures as well as an increase in the I_D/I_G ratio.

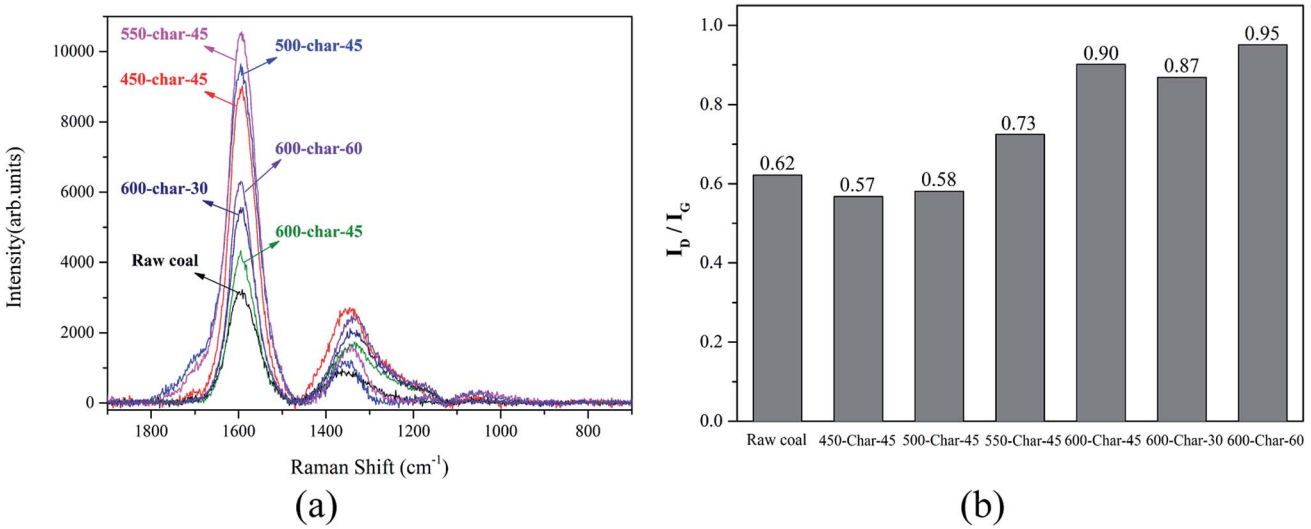

Fig. 1 Raman spectra of the raw coal and char samples (a) and I_D/I_G (b).

Furthermore, the abovementioned process is prolonged with an increase in the holding time, and the I_D/I_G ratio becomes higher. According to the abovementioned analysis, the development of pores in the subsequent activation process is significantly dependent on the structural characteristics of the char, and the char sample with an amorphous structure and less graphite-like carbon is suitable for the preparation of AC. Therefore, the optimal carbonization conditions are as follows: Zhundong coal is heated from room temperature to 600 °C at 5 °C min^{-1} under the protection of N_2 and then maintained at this temperature for 60 min.

However, since few initial pores are produced in the char obtained from the carbonization of Zhundong coal, the char is transformed into AC with a developed pore structure through the activation process. Therefore, all kinds of technical methods to adjust the pore structure of AC finally converged in the activation stage. The formation and development of pores in AC can be regulated by controlling the activation temperature, time, and agent. In this way, fine regulation of the pore structures of AC can be realized.

3.2 Loss on ignition of AC under different activation conditions

After determining the optimal carbonization conditions of Zhundong coal, the pore structure evolution of AC was investigated by changing the activation process conditions such as activation agent, temperature, and holding time. To a certain extent, the loss on ignition (LOI) can reflect the pore structure of AC. Previous studies have suggested that AC with micropores is produced when the LOI is below 50%, and AC with a mixture of macropores and micropores is produced when the LOI is more than 75%.[13] The LOI of the AC sample prepared from Zhundong coal as a function of temperature with H_2O and CO_2 as the activation agents is shown in Fig. 2.

It can be observed from Fig. 2 that whether the activation agent was CO_2 or H_2O, the LOI of AC increased with an increase in temperature in the presence of both H_2O and CO_2, and CO_2 led to a higher LOI change as compared to H_2O. In the case of H_2O, the LOI of AC was less than 50%, which meant that the pore structure of this AC was mainly microporous. During the process of CO_2 activation, the loss on ignition was more than 50% when the temperature was higher than 750 °C, and these phenomena indicated that the amount of macropores in AC gradually increased with an increase in temperature.[13] It can be easily observed that the pore structures of the AC samples prepared by CO_2 and H_2O activation are quite different. The deep reasons for these phenomena will be revealed in the follow-up study.

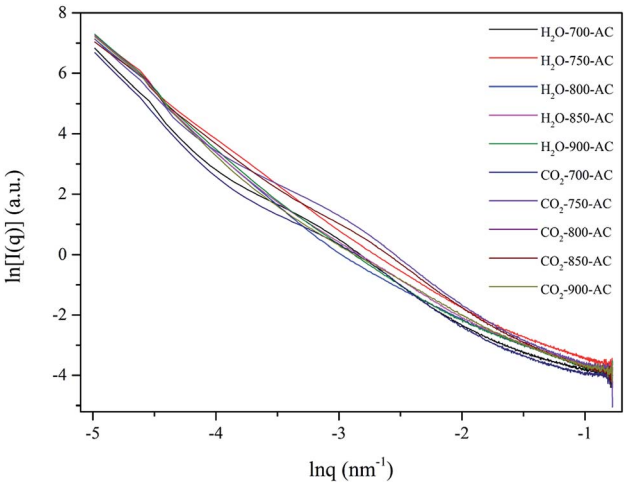

Fig. 3 SAXS logarithmic curves of the different AC samples under different conditions.

3.3 Distribution of the pore structure of AC under different conditions

Maya *et al.*[23] developed a novel mathematical model for coal char activation using H_2O and CO_2, and their results indicated that the H_2O-char reaction increased the pore radius, whereas the CO_2-char reaction increased the pore length. Moreover, they proposed a hypothesis that pore size can be controlled during char activation using the CO_2/H_2O mixture. SAXS can be used to

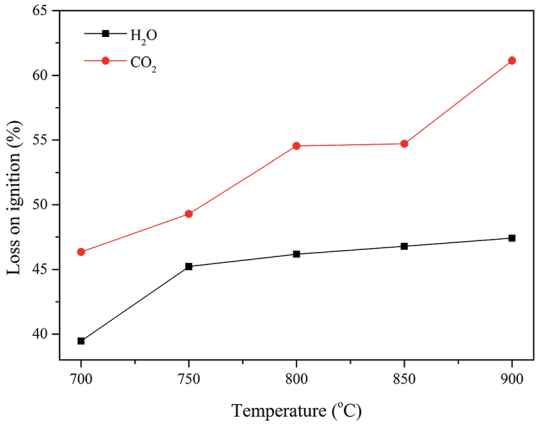

Fig. 2 Loss on ignition of AC under different activation conditions.

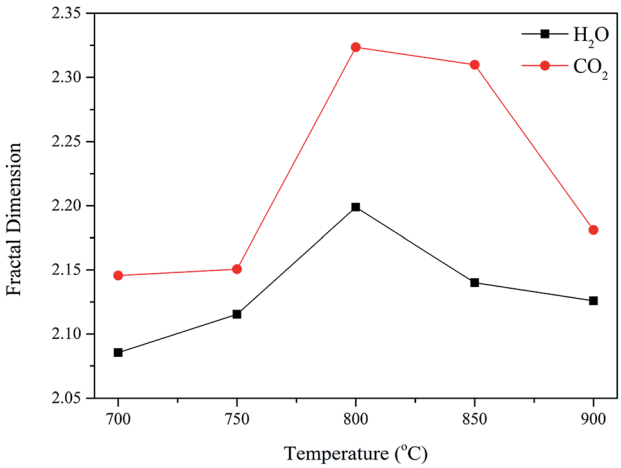

Fig. 4 Fractal dimension of AC under different conditions.

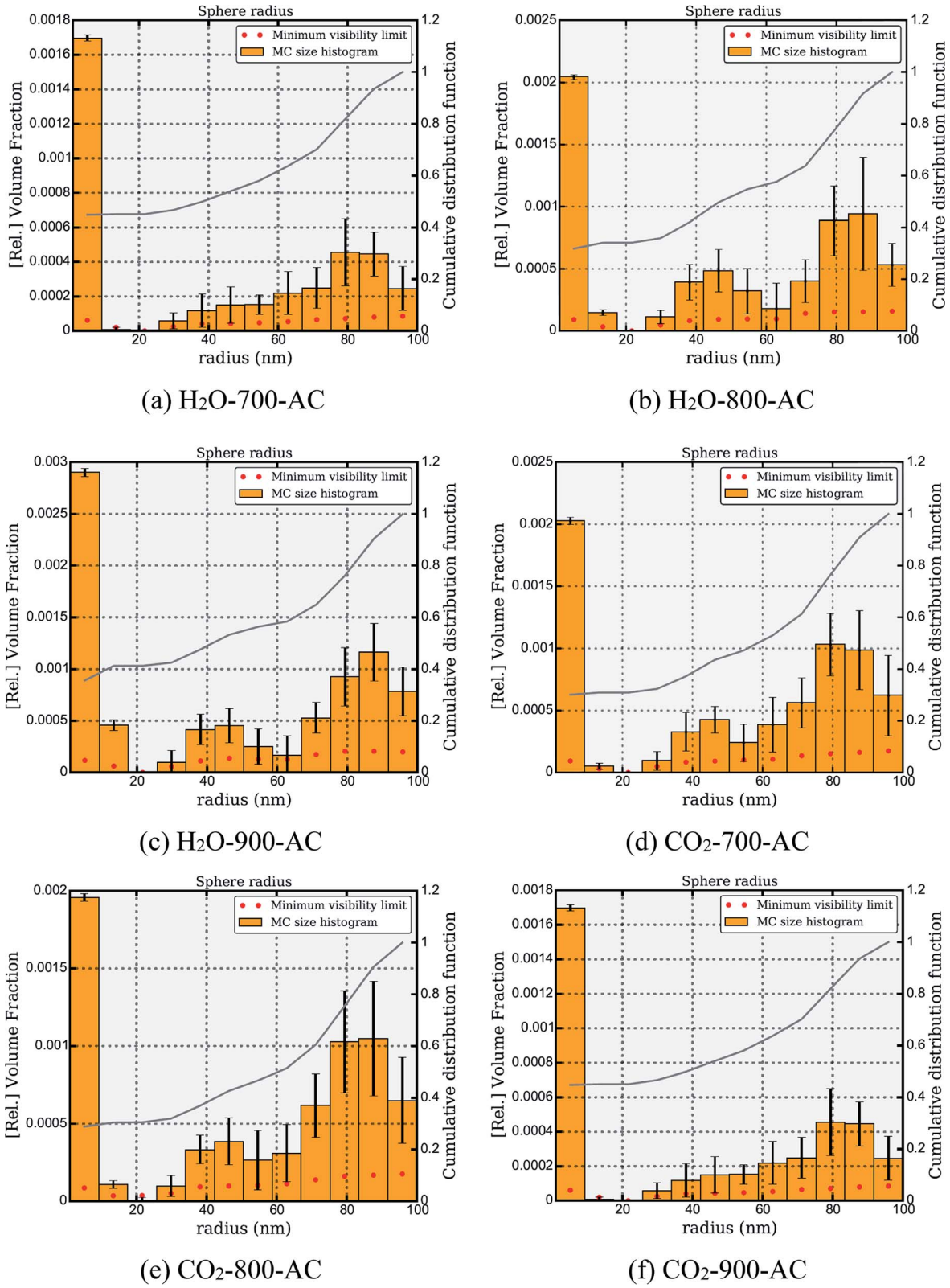

Fig. 5 Variation in the pore size distribution of different AC samples under different conditions. (a) H_2O-700-AC, (b) H_2O-800-AC, (c) H_2O-900-AC, (d) CO_2-700-AC, (e) CO_2-800-AC and (f) CO_2-900-AC.

comprehensively investigate the pore characteristics, such as pore size distribution, specific surface area, and fractal dimension, of carbon materials. Using SAXS, Coetzee *et al.*[24,25] analyzed pore development during the gasification of South African coal with CO_2 or H_2O. They found an increase in the number of pores with an insignificant change in pore size

during the CO_2 gasification; however, for H_2O gasification, an increase in the size of smaller pores was observed with an increase in conversion.

The SAXS technique is used to determine the porosity, pore size distribution, and surface area of carbon materials because it is fast and non-invasive and does not require any complex sample preparation.[26] For this reason, herein, SAXS was used to explore the evolution of the pore structure of AC under different activation conditions. Fractal is a geometrical concept referring to self-similarity and scale invariance; moreover, fractal dimension can quantitatively reflect the irregularity of the material structure, and SAXS is an ideal tool to measure this parameter of the material.[27] The SAXS logarithmic curves of AC under different conditions are shown in Fig. 3. As shown in Fig. 3, there is a significant linear relationship between ln q and ln $I(q)$, where q and $I(q)$ are the scattering vector and scattering intensity, respectively. The results obtained in previous studies have confirmed that if the $I(q)$–q logarithmic curve results in a straight line, the pore size distribution follows fractal behavior.[28] Thus, it was concluded that there was a distinct fractal structure in these AC samples.

In addition, the slopes of these curves are between −3 and −4, which indicate surface fractal in these samples. Then, the fractal dimension could be calculated by eqn (1), and the results are shown in Fig. 4.

$$D_s = 6 + \alpha \quad (1)$$

where α represents the slope of the SAXS logarithmic curve, and D_s is the fractal dimension. The higher the value of D_s, the rougher the surface of the AC samples. As noticed in Fig. 4, the D_s of the AC sample prepared *via* CO_2 activation is higher than that of the AC sample prepared *via* H_2O activation; this suggested that the corrosion and degree of damage to the surface of coal char was stronger in the case of CO_2 than those in the case of H_2O. With an increase in temperature, the D_s of the AC sample prepared by CO_2 or H_2O activation first increased and then decreased. This also reflected that the surface roughness of the AC samples changed with the increasing temperature.

Furthermore, McSAS, a user-friendly open-source Monte Carlo regression package that structures the analysis of the SAXS by scattering contributions,[29] was used to calculate the pore size distribution of AC. As shown in Fig. 5, the variation in the pore size distribution of AC under different conditions was obtained by fitting the SAXS data. The analysis of Fig. 5(a)–(c) revealed that the evolution process of the pore structure of the AC sample derived from H_2O activation and the number of micropores and macropores in this AC sample increased with an increase in temperature. Fig. 5(d)–(f) show that with an increase in temperature, the number of micropores in the AC sample prepared by CO_2 activation increased, whereas that of macropores decreased.

Since the absolute intensity was not calibrated at the SAXS station, the specific surface area of the AC samples could only be characterized by a nitrogen adsorption–desorption analyzer. The effect of temperature on the surface areas of the AC samples prepared by H_2O and CO_2 activation is shown in Fig. 6. According to Fig. 6, the surface area of the AC sample prepared by CO_2 gradually decreased with an increase in temperature. On the contrary, with an increase in temperature, the surface area of the AC sample obtained *via* H_2O activation first increased and reached the highest point at 850 °C; then, with a further increase in temperature, the specific surface area of this AC sample decreased.

Since the activation process is a complex physicochemical process consisting of gas mass-transfer and heterogeneous gas–solid reactions, the evolution of the pore structure of AC was revealed based on the gas–solid diffusion and activation reactions. As is generally known, the molecular size of H_2O is smaller than that of CO_2, and the diffusion resistance of H_2O is significantly lower than that of CO_2.[30,31] Moreover, researchers have confirmed that H_2O more likely diffuses into the pores of coal char than CO_2 during the gasification process.[23,32] Thus, during the activation process, the concentration of CO_2 on the surface of the char was higher than that of H_2O, whereas the situation inside the pores of the char was opposite. By combining these results with the fractal dimension of AC, it could be inferred that the activation of H_2O mainly occurred in the pores of the char, whereas activation of CO_2 occurred on the surface of the char. As a result, the surface of the AC sample prepared by CO_2 activation was rougher than that of the AC sample prepared by H_2O activation.

In addition, the results can be well-explained based on the abovementioned inference. Because of the thermal gradient, the temperature of the pores in the char was lower than that of the surface. When the temperature was 700 °C, H_2O activation mainly occurred in the pores of the char; however, the activation reaction was weak; therefore, the specific surface area of AC was low. In this case, the reaction rate was the main limiting factor for the pore development of AC. With an increase in temperature, the activation reactions in the pores and surface enhanced; then, the surface of AC became rough and the specific surface area increased. With a further increase in temperature, diffusion became the main limiting factor for the pore development of AC. Before the diffusion of H_2O molecules, some H_2O

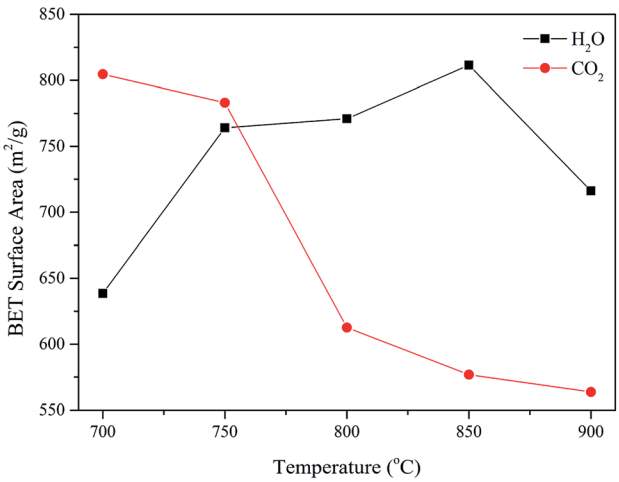

Fig. 6 Effect of temperature on the surface areas of the AC samples prepared by H_2O and CO_2 activation.

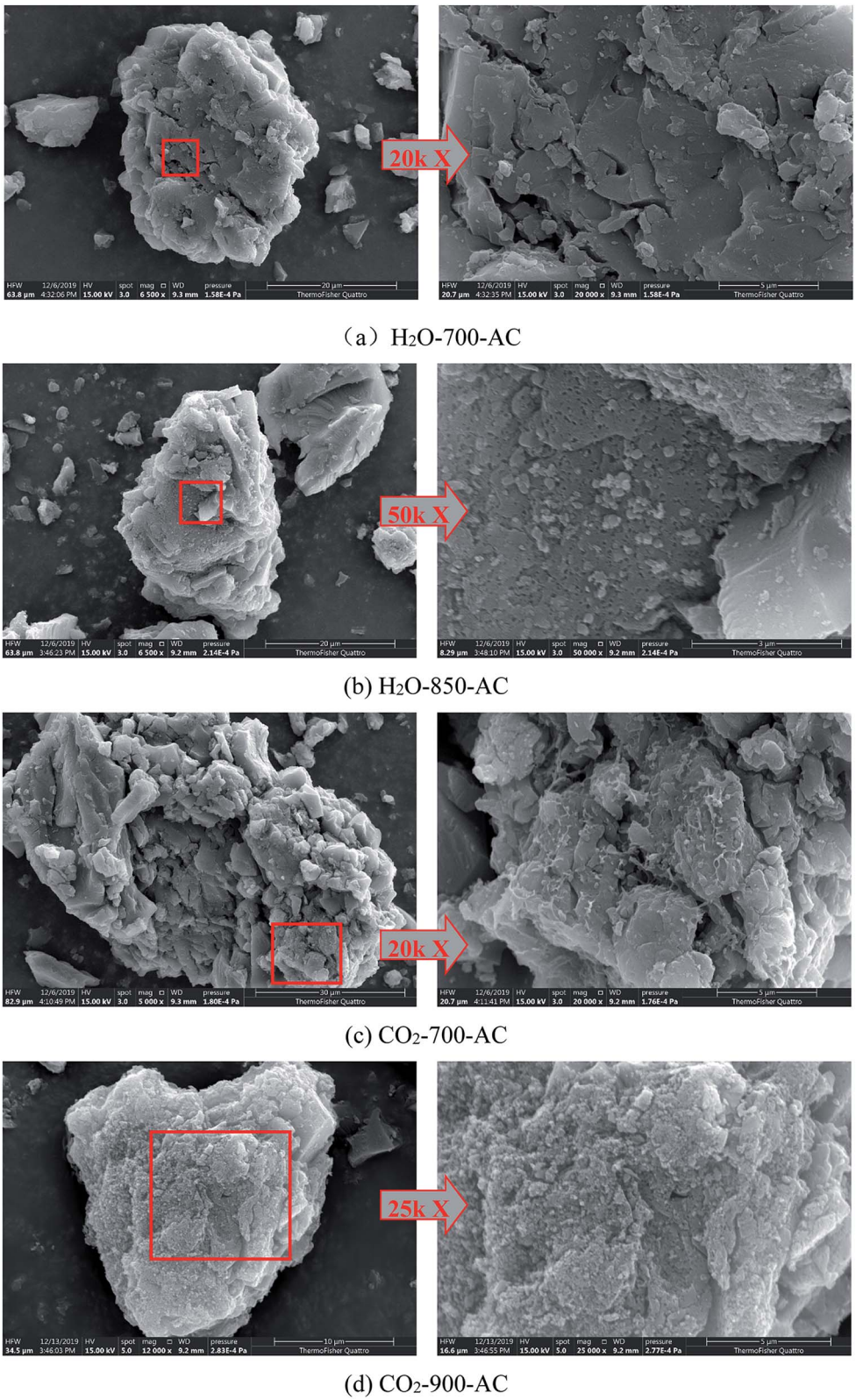

Fig. 7 Surface morphology of AC samples under different conditions. (a) H_2O-700-AC, (b) H_2O-850-AC, (c) CO_2-700-AC and (d) CO_2-900-AC.

molecules were consumed because of the activation reaction, and thus, the H_2O activation reaction mainly occurred on the surface of the char. As a result, a dense surface structure was formed due to the rapid reaction rate, and the fractal dimension and specific surface area of the AC sample were relatively low.

The CO_2 activation reaction mainly occurred on the surface of AC. With the progress of the reaction and the development of

pores on the surface of the char, the diffusion of CO_2 became easier, and then, the pore structure of the prepared AC sample was well-developed. With an increase in the activation temperature, the reaction became faster, and the amount of CO_2 diffused into the pores reduced; this made the surface of the AC sample rough. As a result, the fractal dimension of the prepared AC sample increased, and the specific surface area decreased; especially, the number of micropores decreased, whereas that of macropores increased. With a further increase in temperature, CO_2 was consumed in the activation reaction before its diffusion. Moreover, it was found that the surface of the AC sample prepared at high temperatures was covered with an ash layer during the sampling process. This ash layer hindered the diffusion and activation of CO_2; hence, the surface of the prepared AC sample became smooth, and the specific surface area decreased. Furthermore, because a large amount of carbon matrix was consumed by the CO_2 activation reaction to produce the ash layer, the loss on ignition of the AC sample greatly increased at high temperatures.

By combining these results with the loss on ignition, it can be concluded that the pore structure of Zhundong coal-based AC will be fully developed by H_2O activation at high temperatures or CO_2 activation at low and medium temperatures.

3.4 Changes in the surface morphology of AC under different conditions

ESEM analysis can be used to observe the changes in the surface morphology of AC under different activation conditions. The typical surface images of the AC samples with the highest and lowest specific surface areas are shown in Fig. 7. As shown in Fig. 7(a), it was difficult to observe the trace of the reaction between H_2O and carbon matrix on the surface of H_2O-700-AC; this suggested that at low temperatures, the H_2O activation reaction mainly occurred in the pores of the char, and the diffusion of H_2O occurred prior to the activation reaction. When the temperature was increased to 850 °C, a large number of pores appeared on the surface of H_2O-850-AC, as depicted in Fig. 7(b); this indicated that H_2O reacted with the carbon matrix on the surface of AC at high temperatures, and these pores substantially improved the specific surface area of AC. This also suggested that the H_2O activation reaction was preferred over H_2O diffusion. Fig. 7(c) shows the surface morphology of the AC sample prepared from the char activated by CO_2 at 700 °C, and the trace of the reaction between CO_2 and carbon matrix on the surface of the char could be clearly found. It was inferred that the activation reaction of CO_2 on the surface of the char was more strong than that of H_2O at relatively low temperatures. As observed from Fig. 7(d), CO_2 reacted with the carbon matrix on

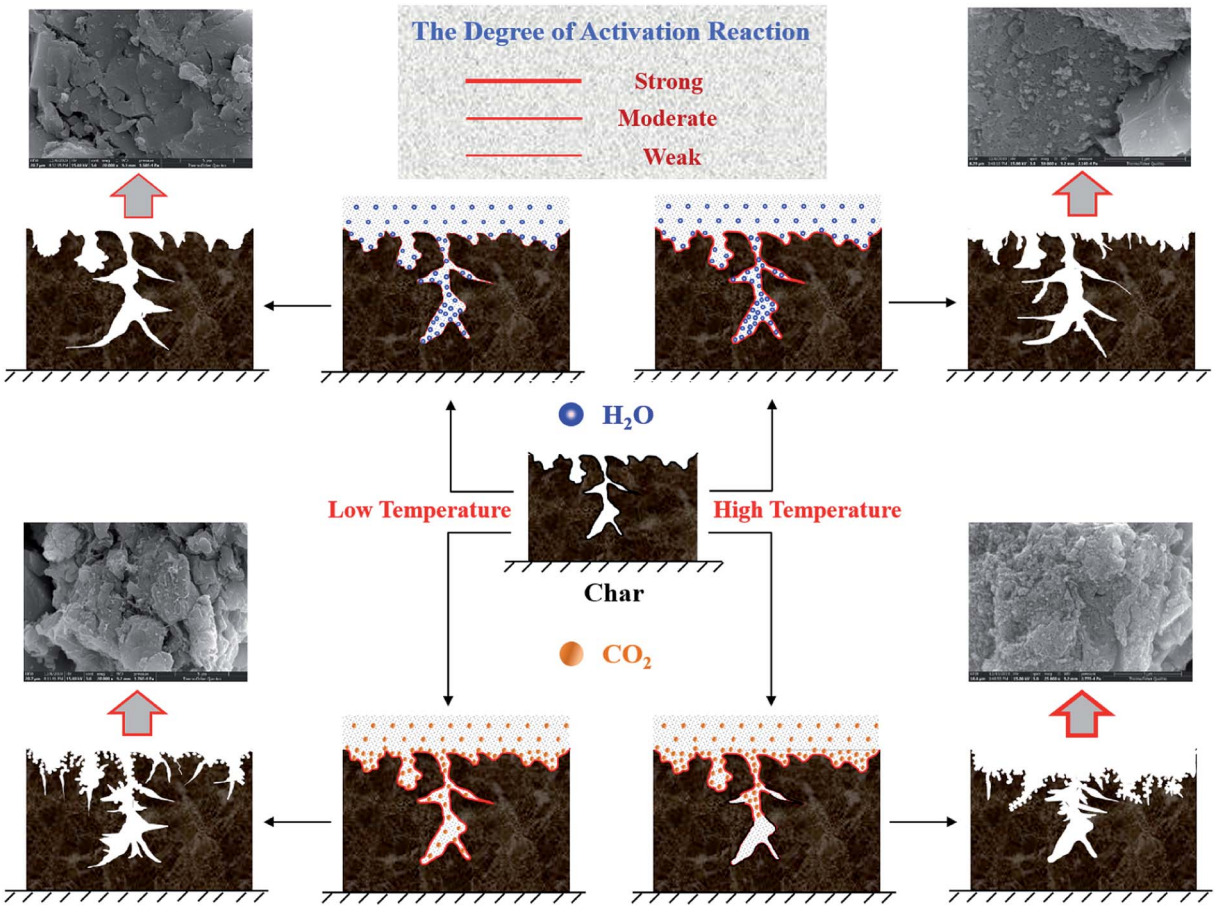

Fig. 8 Mechanism of the evolution of the pore structure of the AC samples prepared under different conditions.

the surface of the char roughly at 900 °C, and AC with a dense surface was formed. Therefore, the fractal dimension and specific surface area of the prepared AC sample reduced. Overall, the ESEM results indirectly proved the effects of H_2O and CO_2 activation on the pore structure development of AC at different activation temperatures.

3.5 Mechanism of the evolution of the pore structure of AC under different conditions

According to the abovementioned results, the evolution mechanism of the pore structure of AC during H_2O and CO_2 activation was inferred, as shown in Fig. 8. At low temperatures, H_2O diffuses into the pores of the char because the diffusion of H_2O is preferred over the activation reaction. Due to the existence of a temperature gradient, the temperature inside the char is lower than that of the surface,[33] and the internal activation reaction is weak. Consequently, the pore development of the prepared AC sample is poor. On the contrary, the concentration of CO_2 on the surface of the char is high because of the weak diffusion of CO_2. These CO_2 molecules react with the carbon matrix on the surface of the char and produce some pores, which improve the diffusion of CO_2 inside the char. Therefore, the pores of the prepared AC sample are fully developed. At high temperatures, the H_2O activation reaction is no longer limited by the reaction rate, and H_2O reacts with the carbon matrix while diffusing; this makes the internal pores well-developed. The CO_2 activation reaction rate enhances with an increase in temperature; this leads to the consumption of CO_2 *via* reaction with the carbon matrix before its diffusion inside the char, and then, the diffusion-limited activation of CO_2 is intensified. Moreover, the surface of the char is covered with an ash layer due to the strong CO_2 activation reaction, and the ash layer further hinders the diffusion of CO_2 inside the char.[34] Thus, these factors lead to the formation of an AC sample with a dense surface and poor pore structure.

As abovementioned, researchers have proposed a hypothesis that the development of pore structure can be regulated to occur in a certain way during the preparation of activated carbon.[13,23] In this study, it was proven that pore formation shows distinct characteristics during the H_2O and CO_2 activation processes. Therefore, proper utilization of the unique characteristics of H_2O and CO_2 during pore formation is important to control the entire activation process and realize the preparation of AC with a specific pore structure. In addition, the high content of AAEMs in Zhundong coal can significantly reduce the activation temperature; thus, the preparation of high value-added porous carbon material is a promising approach for the clean utilization of Zhundong coal.

4. Conclusion

The preparation of AC from Zhundong high-alkali coal requires low carbonization and activation temperatures as well as the presence of a carbon matrix, which can effectively inhibit the volatilization of AAEMs. Moreover, the residual AAEMs can significantly reduce the activation temperature and promote the development of the pore structure; thus, the preparation of high-value-added porous carbon materials is a promising approach for the clean utilization of Zhundong high-alkali coal.

According to the carbonization control theory, the char with an amorphous structure and less graphite-like carbon, obtained by heating Zhundong high-alkali coal from room temperature to 600 °C at 5 °C min^{-1} and then maintaining the acquired product at this temperature for 60 min, is suitable for the subsequent activation process.

Based on the idea of decoupling, the activation process was divided into gas–solid diffusion and activation reactions, and the mechanism of the evolution of the pore structure of AC prepared by the activation of H_2O and CO_2 at different temperatures was revealed. At low temperatures, the process of H_2O activation is dominated by H_2O diffusion, and the weak reaction results in a poor development of the pore structure of AC. Then, with an increase in temperature, the activation of H_2O is enhanced and the pore structure of AC is fully developed. Due to the poor diffusion of CO_2, the CO_2 activation reaction mainly occurs on the surface of the char at low temperatures, and then, the pores produced on the surface of the char can improve the diffusion of CO_2 such that the pore structure of the AC develops well. With an increase in temperature, the diffusion of CO_2 is reduced by the enhancement of CO_2 activation; this leads to the consumption of the carbon matrix by CO_2 gasification instead of pore formation by the CO_2 activation reaction. Thus, proper utilization of the unique characteristics of H_2O and CO_2 during pore formation is important to regulate the activation process and realize the preparation of AC with a specific pore structure.

Conflicts of interest

The authors declare that they have no known competing financial interests or personal relationships that could have appeared to influence the work reported in this paper.

Acknowledgements

The authors gratefully thank Prof. Zhihong Li of Beijing Synchrotron Radiation Facility, Institute of High Energy Physics for his help in SAXS data processing. This work was financially supported by the National Key Research and Development Program of China (2016YFB0600305).

References

1 H. Zhang, X. Guo and Z. Zhu, Effect of temperature on gasification performance and sodium transformation of Zhundong coal, *Fuel*, 2017, **189**, 301–311.
2 J. Zhou, X. Zhuang, A. Alastuey, *et al.*, Geochemistry and mineralogy of coal in the recently explored Zhundong large coal field in the Junggar basin, Xinjiang province, China, *Int. J. Coal Geol.*, 2010, **82**(1), 51–67.
3 C. Z. Li, Some recent advances in the understanding of the pyrolysis and gasification behaviour of Victorian brown coal, *Fuel*, 2007, **86**, 1664–1683.

4 D. Liang, Q. Xie, C. Wan, *et al.*, Evolution of structural and surface chemistry during pyrolysis of Zhundong coal in an entrained-flow bed reactor, *J. Anal. Appl. Pyrolysis*, 2019, **140**, 331–338.
5 D. Liang, Q. Xie, H. Zhou, *et al.*, Catalytic effect of alkali and alkaline earth metals in different occurrence modes in Zhundong coals, *Asia-Pac. J. Chem. Eng.*, 2018, **13**, 2190.
6 C. Zhu, S. Qu, J. Zhang, *et al.*, Distribution, occurrence and leaching dynamic behavior of sodium in Zhundong coal, *Fuel*, 2017, **190**, 189–197.
7 R. Kumar, R. K. Singh, A. K. Ghosh, *et al.*, Synthesis of coal-derived single-walled carbon nanotube from coal by varying the ratio of Zr/Ni as bimetallic catalyst, *J. Nanoparticle Res.*, 2013, **15**, 1406.
8 J. Rizkiana, G. Guan, W. B. Widayatno, *et al.*, Promoting effect of various biomass ashes on the steam gasification of low-rank coal, *Appl. Energy*, 2014, **133**, 282–288.
9 R. Li, Q. Chen and H. Xia, Study on pyrolysis characteristics of pretreated high-sodium (Na) Zhundong coal by skimmer-type interfaced TG-DTA-EI/PI-MS system, *Fuel Process. Technol.*, 2018, **170**, 79–87.
10 Y. Gao, L. Ding, X. Li, *et al.*, Na & Ca removal from Zhundong coal by a novel CO_2-water leaching method and the ashing behavior of the leached coal, *Fuel*, 2017, **210**, 8–14.
11 D. Liang, Q. Xie, Z. Wei, *et al.*, Transformation of alkali and alkaline earth metals in Zhundong coal during pyrolysis in an entrained flow bed reactor, *J. Anal. Appl. Pyrolysis*, 2019, 104661.
12 Z. Ma, J. Bai, X. Wen, *et al.*, Mineral Transformation in Char and Its Effect on Coal Char Gasification Reactivity at High Temperatures Part 3: Carbon Thermal Reaction, *Energy Fuels*, 2014, **28**(5), 3066–3073.
13 Q. Xie, X. Zhang, L. Li, *et al.*, Porosity adjustment of activated carbon theory approaches and practice, *N. Carbon Mater.*, 2005, **20**(2), 183–190.
14 X. Y. Zhang, B. Gao, A. E. Creamer, *et al.*, Adsorption of VOCs onto engineered carbon materials: a review, *J. Hazard. Mater.*, 2017, **338**(15), 102–123.
15 R. L. Tseng, S. K. Tseng, F. C. Wu, *et al.*, Effects of micropore development on the physicochemical properties of KOH-activated carbons, *J. Chin. Inst. Chem. Eng.*, 2008, **39**, 37–47.
16 E. Cetin, B. Moghtaderi, R. Gupta, *et al.*, Influence of pyrolysis conditions on the structure and gasification reactivity of biomass chars, *Fuel*, 2004, **83**(16), 2139–2150.
17 D. Liang, Q. Xie, G. Li, *et al.*, Influence of heating rate on reactivity and surface chemistry of chars derived from pyrolysis of two Chinese low rank coals, *Int. J. Min. Sci. Technol.*, 2018, **28**(4), 613–619.
18 X. Zhang, C. Zhang, P. Tan, *et al.*, Effects of hydrothermal upgrading on the physicochemical structure and gasification characteristics of Zhundong coal, *Fuel Process. Technol.*, 2018, **172**, 200–208.
19 R. Kumar, R. K. Singh, P. K. Dubey, *et al.*, Highly zone-dependent synthesis of different carbon nanostructures using plasma-enhanced arc discharge technique, *J. Nanoparticle Res.*, 2015, **17**, 24.
20 L. Zhang, T. Li, S. Wang, *et al.*, Changes in char structure during the thermal treatment of nascent chars in N_2 and subsequent gasification in O_2, *Fuel*, 2017, **199**, 264–271.
21 X. Li, J. Hayashi and C. Li, FT-Raman spectroscopic study of the evolution of char structure during the pyrolysis of a Victorian brown coal, *Fuel*, 2006, **85**, 1700–1707.
22 R. Kumar, R. K. Singh, P. K. Dubey, *et al.*, Pressure-dependent synthesis of high-quality few-layer graphene by plasma-enhanced arc discharge and their thermal stability, *J. Nanoparticle Res.*, 2013, **15**, 1847.
23 J. C. Maya, R. Macias, C. A. Gomez, *et al.*, On the evolution of pore microstructure during coal char activation with steam/CO_2 mixtures, *Carbon*, 2020, **158**, 121–130.
24 G. H. Coetzee, R. Sakurovs, H. W. J. P. Neomagus, *et al.*, Pore development during gasification of South African inertinite-rich chars evaluated using small angle X-ray scattering, *Carbon*, 2015, **95**, 250–260.
25 G. H. Coetzee, R. Sakurovs, H. W. J. P. Neomagus, *et al.*, Particle size influence on the pore development of nanopores in coal gasification chars: from micron to millimeter particles, *Carbon*, 2017, **112**, 37–46.
26 F. Xie, Z. Li, W. Wang, *et al.*, In situ SAXS study of pore structure during carbonization of non-caking coal briquettes, *Fuel*, 2020, **262**, 116547.
27 R. Diduszko, A. Swiatkowski and B. J. Trznadel, On surface of micropores and fractal dimension of activated carbon determined on the basis of adsorption and SAXS investigations, *Carbon*, 2000, **38**(8), 1153–1162.
28 T. Nakagawa, I. Komaki, M. Sakawa, *et al.*, Small angle X-ray scattering study on change of fractal property of Witbank coal with heat treatment, *Fuel*, 2000, **79**(11), 1341–1346.
29 I. Bressler, B. R. Pauw and A. F. Thunemann, McSAS: software for the retrieval of model parameter distributions from scattering patterns, *J. Appl. Crystallogr.*, 2015, **48**(3), 962–969.
30 J. Chen, W. Chen, R. Ji, *et al.*, Kinetic studies on bituminous coal char gasification using CO_2 and H_2O mixtures, *Int. J. Green Energy*, 2019, **16**(14), 1144–1151.
31 S. Umemoto, S. Kajitani and S. Hara, Modeling of coal char gasification in coexistence of CO_2 and H_2O considering sharing of active sites, *Fuel*, 2013, **103**, 14–21.
32 C. Guizani, F. J. Escudero Sanz and S. Salvador, Influence of temperature and particle size on the single and mixed atmosphere gasification of biomass char with H_2O and CO_2, *Fuel Process. Technol.*, 2015, **134**, 175–188.
33 Y. J. Wang, X. M. Zhang, H. M. Zhang, *et al.*, Effects of temperature gradient and particle size on self-ignition temperature of low-rank coal excavated from inner Mongolia, China, *R. Soc. Open Sci.*, 2019, **6**(9), 190374.
34 M. Liu, Z. J. Shen, Q. F. Liang, *et al.*, Morphological evolution of a single char particle with a low ash fusion temperature during the whole gasification process, *Energy Fuels*, 2018, **32**(2), 1550–1557.